

## A study of magnetoelectric domain formation in $\text{Cr}_2\text{O}_3$

This article has been downloaded from IOPscience. Please scroll down to see the full text article.

1998 J. Phys.: Condens. Matter 10 663

(<http://iopscience.iop.org/0953-8984/10/3/017>)

View [the table of contents for this issue](#), or go to the [journal homepage](#) for more

Download details:

IP Address: 171.66.16.209

The article was downloaded on 14/05/2010 at 12:00

Please note that [terms and conditions apply](#).

## A study of magnetoelectric domain formation in $\text{Cr}_2\text{O}_3$

P J Brown<sup>†</sup>, J B Forsyth<sup>‡</sup> and F Tasset<sup>†</sup>

<sup>†</sup> Institut Laue–Langevin, BP 156 38042, Grenoble Cédex, France

<sup>‡</sup> Rutherford Appleton Laboratory, Chilton, Oxon OX11 0QX, UK

Received 10 October 1997

**Abstract.** The newly developed technique of zero-field neutron polarimetry has been used to determine the imbalance in the population of  $180^\circ$  domains in antiferromagnetic  $\text{Cr}_2\text{O}_3$  produced by cooling through the Néel temperature under different conditions. The method allows the absolute spin configuration of the preferred domain to be determined. In the structure of  $\text{Cr}_2\text{O}_3$  the  $\text{Cr}^{3+}$  ions are distributed along the trigonal axes in pairs across the centres of symmetry; in the antiferromagnetic phase their moments are aligned parallel and antiparallel to this axis. It is found that although a magnetic field applied parallel to this axis during cooling is able to change the domain populations, these changes are neither reversible nor completely predictable. On the other hand, cooling with combined electric and magnetic fields along the trigonal axis leads to much more consistent results, and virtually single-domain crystals of either type can be obtained. The type of domain produced depends on whether the electric and magnetic fields are parallel or antiparallel. When the sample is cooled in parallel fields, the domain produced is that in which the magnetic moments on the  $\text{Cr}^{3+}$  ions of each closely spaced pair point towards one another. The different atomic perturbations which lead to a magnetoelectric effect are discussed and it is shown that the  $g$ -factor process can give the observed magnetoelectric annealing effect.

### 1. Introduction

A linear magnetoelectric (ME) effect in which magnetization can be induced by the application of an electric field can only exist in crystals with ordered magnetic structures having particular magnetic symmetries [1]. A necessary feature is a magnetic structure with zero propagation vector; then, if the magnetic structure also contains a centre of symmetry combined with time inversion, an ME effect can exist [2]. The magnetic moments in such structures can order in one or other of two  $180^\circ$  domains which differ because the magnetic moments have opposite directions with respect to the arrangement of their ligand atoms. Such domains can only be transformed into one another by the time-reversal operation and not by any spatial rotation or inversion.

Experiments by Astrov, Rado and others [3–6] have shown that although the ME susceptibilities of  $\text{Cr}_2\text{O}_3$  have a unique temperature dependence, their magnitudes and even their signs are specimen dependent. Rado and Folen [7] attributed this specimen dependence to the existence of  $180^\circ$  antiferromagnetic domains which have opposite ME effects. It was suggested that enhancement of the ME effect by cooling through the Néel temperature in a static magnetic field, and its virtual erasure after cooling in an alternating field was due to the production of single and equi-domain states, respectively.  $\text{Cr}_2\text{O}_3$  has the corundum structure in which the chromium is octahedrally coordinated by oxygen atoms. The Cr sites are not centres of symmetry, so the triad axis of the octahedron is polar. In the antiferromagnetic state the Cr spins are parallel to the triad axis, atoms with opposite spins

being related by the centres of symmetry. In structural terms the  $180^\circ$  domains referred to above are distinguished by the direction in which the spins point relative to the polar axis of their coordinating octahedron. We have shown in previous experiments [8] that neutron polarimetry can be used to determine the domain populations in a particular specimen and can indicate the absolute configuration of the predominant domain. We have now investigated the longitudinal ME effect in  $\text{Cr}_2\text{O}_3$  and determined which of the two magnetic configurations is stabilized by cooling a sample through its Néel point, first with parallel and then with antiparallel magnetic and electric fields applied along the triad axis.

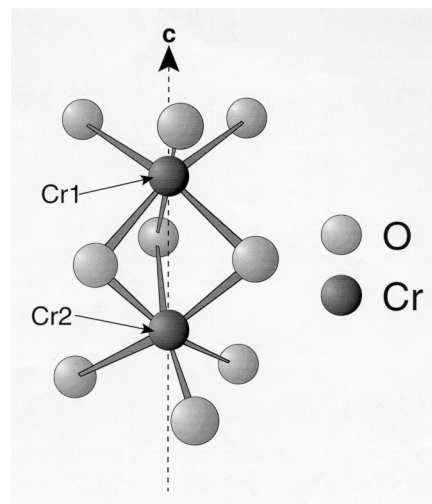


**Figure 1.** The local coordination of the two types of  $\text{Cr}^{3+}$  ion in  $\text{Cr}_2\text{O}_3$ . The upper  $\text{Cr}^{3+}$  ion is Cr1 and the lower Cr2.

**Table 1.** Crystallographic data for  $\text{Cr}_2\text{O}_3$ .

Space group: $R\bar{3}c$ , hexagonal axes			
Unit cell: $a = 4.9607 \text{ \AA}$ , $c = 13.599 \text{ \AA}$			
Atomic positions:	12 Cr in 12(c)	$0\ 0\ z$	$z = 0.3476$
	18 O in 18(e)	$x\ 0\ \frac{1}{4}$	$x = 0.3056$

## 2. The crystal and magnetic structure of $\text{Cr}_2\text{O}_3$

$\text{Cr}_2\text{O}_3$  has the rhombohedral corundum structure, space group  $R\bar{3}c$ . We shall describe it within this paper in terms of hexagonal axes. The crystallographic data are given for reference in table 1. Each  $\text{Cr}^{3+}$  ion has six  $\text{O}^{2-}$  neighbours. The three nearest ( $1.965 \text{ \AA}$ ) form an equilateral triangle of edge  $2.99 \text{ \AA}$  in a plane perpendicular to  $c$ . The other three are slightly further away ( $2.016 \text{ \AA}$ ), and form a similar but smaller triangle, edge  $2.63 \text{ \AA}$ , again perpendicular to  $c$  but on the other side of the  $\text{Cr}^{3+}$  ion. The  $\text{CrO}_6$  octahedra are joined in pairs sharing their smaller triangular faces as illustrated in figure 1. The vertices of the shared triangles are also vertices of the large triangular faces of two other such double octahedra. Thus each  $\text{O}^{2-}$  ion has four  $\text{Cr}^{3+}$  neighbours.

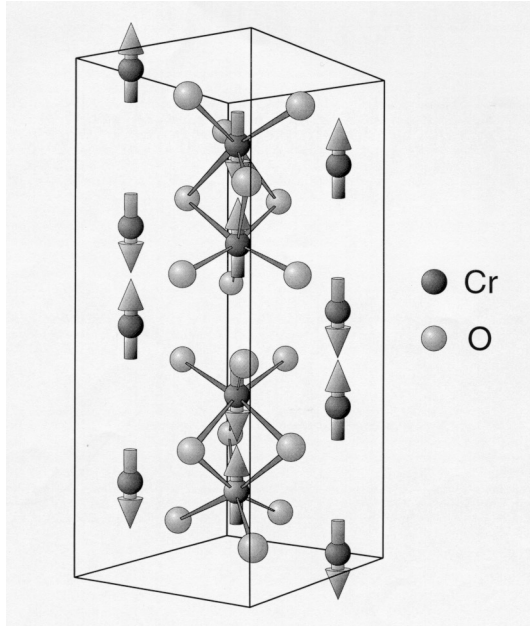


**Figure 2.** The magnetic structure of  $\text{Cr}_2\text{O}_3$ . The domain which is illustrated is that which is stabilized when the crystal is cooled in electric and magnetic fields applied parallel to  $c$  which have the same sense.

$\text{Cr}_2\text{O}_3$  undergoes a transition from a paramagnetic to an antiferromagnetic structure at 310(2) K. The antiferromagnetic structure has zero propagation vector and can be described in the magnetic space group  $R\bar{3}c'$  [9]; it is illustrated in figure 2. The  $\text{Cr}^{3+}$  spins have the sequence  $+ - + -$  along the trigonal axis and are parallel to it [10]. Because the  $\text{Cr}^{3+}$  ions of opposite spin are related by a centre of symmetry their coordinating octahedra are inverted. It will be convenient to be able to distinguish these two types of site, so those in the upper octahedron of the double complex will be identified as Cr1 and those in the lower as Cr2.

### 3. Magnetic scattering by $\text{Cr}_2\text{O}_3$

The interaction vectors for magnetic scattering by  $\text{Cr}_2\text{O}_3$  have the form

$$\mathbf{Q}_{hk,\ell} = 12M_{\text{Cr}}f_{\text{Cr}}(\kappa) i \sin(2\pi\ell z)(\hat{\kappa} \times \hat{c} \times \hat{\kappa}) \quad \text{for } \ell \text{ even} \quad (1)$$

and are zero for  $\ell$  odd.  $M_{\text{Cr}}$  is the  $\text{Cr}^{3+}$  magnetic moment,  $f_{\text{Cr}}(\kappa)$  its form factor and  $z$  its positional parameter.  $\kappa$  is the scattering vector of the  $hk,\ell$  reflection, and  $\hat{\kappa}$  and  $\hat{c}$  are unit vectors parallel to  $\kappa$  and the  $c$ -axis respectively. The magnetic interaction vectors are pure imaginary ( $\mathbf{Q} = -\mathbf{Q}^*$ ) and lie at right angles to  $\kappa$  in the plane containing  $\kappa$  and  $c$ . For elastic scattering by a Bragg reflection which contains both nuclear and magnetic contributions, the expression given by Blume [11] for the scattered polarization can be written as

$$\begin{aligned} \mathbf{P}' \frac{\partial \sigma}{\partial \omega} = & \mathbf{P}(NN^* - \mathbf{Q} \cdot \mathbf{Q}^*) + 2\Re(\mathbf{Q}N^* + \mathbf{Q}(\mathbf{P} \cdot \mathbf{Q}^*)) \\ & + 2\mathbf{P} \times \Im(\mathbf{Q}N^*) + i(\mathbf{Q} \times \mathbf{Q}^*) \end{aligned} \quad (2)$$

where  $N$  is the nuclear structure factor,  $\mathbf{Q}$  the magnetic interaction vector, and  $\mathbf{P}$  and  $\mathbf{P}'$  are the incident and scattered polarizations respectively. The partial differential cross-section

$$\frac{\partial \sigma}{\partial \omega} = NN^* + \mathbf{Q} \cdot \mathbf{Q}^* + 2\mathbf{P} \cdot \Re(\mathbf{Q}N^*) + i\mathbf{P} \cdot (\mathbf{Q}^* \times \mathbf{Q}). \quad (3)$$

When  $N$  is real and  $\mathbf{Q}$  imaginary, as they are for  $\text{Cr}_2\text{O}_3$ , equations (2) and (3) reduce to

$$\mathbf{P}'(1 + \gamma^2) = \mathbf{P}(1 - \gamma^2) + 2\gamma^2 \hat{\mathbf{q}}(\mathbf{P} \cdot \hat{\mathbf{q}}) + 2\gamma(\mathbf{P} \times \hat{\mathbf{q}}) \quad (4)$$

where  $\hat{\mathbf{q}}$  is a unit vector parallel to  $\hat{\mathbf{k}} \times \hat{\mathbf{c}} \times \hat{\mathbf{k}}$  and  $\gamma \hat{\mathbf{q}} = \Im(\mathbf{Q})/N$ . In considering the scattering from any particular reflection it is convenient to define a set of orthogonal *polarization axes* such that  $z$  is vertical (perpendicular to the scattering plane),  $x$  is parallel to the scattering vector and  $y$  completes a right-handed set. With this definition there can be no component of  $\mathbf{Q}$  parallel to  $x$ . If the  $\text{Cr}_2\text{O}_3$  crystal is aligned with its  $c$ -axis in the scattering plane then  $Q_z = 0$  and  $\mathbf{Q}$  is parallel or antiparallel to  $y$  for all scattering vectors in the horizontal plane. The results of polarimetry experiments can be described by the tensor equation

$$P'_i = \mathbf{P}_{ij} P_j + P''_j$$

where  $\mathbf{P}$  is a tensor describing the rotation of the polarization in the scattering process and  $\mathbf{P}''$  is the polarization created. In the present case no terms which create polarization are present so  $\mathbf{P}'' = 0$  and using equation (4)

$$\begin{aligned} \mathbf{P}_{xx} &= \beta & \mathbf{P}_{yx} &= 0 & \mathbf{P}_{zx} &= -\xi \\ \mathbf{P}_{xy} &= 0 & \mathbf{P}_{yy} &= 1 & \mathbf{P}_{zy} &= 0 \\ \mathbf{P}_{xz} &= \xi & \mathbf{P}_{yz} &= 0 & \mathbf{P}_{zz} &= \beta \end{aligned} \quad (5)$$

with

$$\xi = \frac{2q_y \gamma}{1 + \gamma^2} \quad \text{and} \quad \beta = \frac{1 - \gamma^2}{1 + \gamma^2}. \quad (6)$$

$q_y$  is +1 if  $\hat{\mathbf{q}}$  is parallel to  $y$  and -1 if it is antiparallel. The two  $180^\circ$  domains are derived from one another by reversing all of the spin directions so that their magnetic interaction vectors are equal but opposite; their nuclear structure factors are however the same. The net effect is to change the sign of  $\gamma$ . If the volumes of crystal belonging to the two domains are  $v^+$  and  $v^-$ , a domain ratio  $\eta = (v^+ - v^-)/(v^+ + v^-)$  can be defined. Summing the scattered polarization weighted by its intensity over the two domains gives

$$\begin{aligned} \mathbf{P}_{xx} &= \beta & \mathbf{P}_{yx} &= 0 & \mathbf{P}_{zx} &= -\eta \xi \\ \mathbf{P}_{xy} &= 0 & \mathbf{P}_{yy} &= 1 & \mathbf{P}_{zy} &= 0 \\ \mathbf{P}_{xz} &= \eta \xi & \mathbf{P}_{yz} &= 0 & \mathbf{P}_{zz} &= \beta. \end{aligned} \quad (7)$$

For an equi-domain crystal  $\eta = 0$ , the matrix is diagonal and the incident and scattered polarizations are always parallel. Depolarization by the factor  $\beta$  occurs for incident polarization parallel to either  $x$  or  $z$ , but a beam polarized parallel to  $y$  (the direction of the interaction vector) is always scattered without change of polarization. The signature of a crystal containing unequal volumes of the two domains is rotation of the scattered polarization in the  $x$ - $z$  plane, the direction of rotation indicating which domain is predominant. From the form of the factors  $\xi$  and  $\beta$  in equation (6) it can be seen that the polarization is most sensitive to the domain ratio when  $\gamma = \pm 1$ , since then  $\xi = \pm 1$  and  $\beta = 0$ : an equi-domain crystal will completely depolarize the beam and a single-domain sample will rotate the polarization by  $90^\circ$ . For this reason we have done most of our experiments using the  $\{10\cdot 2\}$  reflections of  $\text{Cr}_2\text{O}_3$  for which  $\gamma = 1$  at  $\approx 290$  K.

#### 4. Experiments

The first series of zero-field neutron polarimetry experiments was carried out using CRYOPAD I [8]; subsequent experiments were carried out with CRYOPAD II [12]. Both were mounted on the polarized neutron inelastic spectrometer IN20 at the Institut Laue–Langevin, Grenoble. The incident wavelength was 1.53 Å and the analyser was set to accept elastic scattering.

In the first series of neutron polarimetric experiments we determined the domain ratios produced in two different single crystals of  $\text{Cr}_2\text{O}_3$  by cooling them through the Néel temperature of 310 K in a static magnetic field of 1.7 T provided by an electromagnet placed outside the experimental zone of IN20. In these exploratory experiments the sample was not in a container so that it could be heated easily to above the Néel temperature using a hand-held hot-air blower. It was then allowed to cool to room temperature by natural convection, or alternatively it was quenched using a stream of cold nitrogen gas; in neither case could the actual rate of cooling be measured or controlled. The sample environment was improved for the experiments made on CRYOPAD II in which there is a large (192 mm diameter) cylindrical region into which the crystal and its sample environment can be introduced. For these experiments the crystal was mounted on an aluminium support whose temperature could be controlled in the range 270–317 K by an electrical heating element and a thermoelectric cooler. Both crystals were in the form of plates cut perpendicular to the triad axis and their flat faces were coated with silver conducting paint which could be connected to a regulated high-voltage DC power supply.

After each field cooling the crystal was transferred to the CRYOPAD, its orientation about the vertical axis of rotation re-established and its temperature set to 290 K before we measured the polarization scattered with incident polarization in the six cardinal directions ( $x, y, z, -x, -y, -z$ ) on the polarization axes defined in the previous section.

#### 5. Results

The most significant findings obtained using CRYOPAD I and magnetic field cooling only were as follows.

(i) Initially, one of the crystals was close to being mono-domain with a domain ratio  $\eta = 0.9$ . The preferred domain could be switched by heating to 315 K and recooling first in one direction of magnetic field and then in the other. The second crystal started out with the same domain preference, but with a much smaller domain imbalance,  $\eta \approx 0.25$ , which could also be switched in the same way.

(ii) Quenching produced an equi-domain sample, as did slow cooling with the field in the basal plane.

(iii) Subsequent slow cooling with the field along [00.1] produced a varying degree of domain imbalance in both crystals, but  $\eta$  never exceeded 0.3 once a crystal had been made equi-domain. Since the same value of magnetic field was used in each experiment, this variability is ascribed to a variation in the actual rate of cooling through the critical temperature of 310 K. This temperature is close enough to ambient for stray air currents to influence the result. However, the same preferred domain was always produced by a given field direction and this preference was reversed each time the field direction was reversed.

The crucial role played by the presence of both a magnetic and an electric field in producing a mono-domain sample was established using CRYOPAD II. Although an electric field of some  $750 \text{ V mm}^{-1}$  did not by itself influence the domain ratio of the crystal during

field cooling or when applied at 290 K, it gave rise to nearly mono-domain samples when employed in conjunction with a magnetic field of 0.68 T during field cooling. For a given direction of magnetic field, the preferred domain could be reversed by reversing the direction of the electric field and vice versa.

**Table 2.** Values of scattered polarization measured for  $\{10\bar{2}\}$  reflections of  $\text{Cr}_2\text{O}_3$  at  $T \approx 290$  K after cooling through the Néel temperature in combined magnetic and electric fields of 1.7 T and  $3500 \text{ V cm}^{-1}$  parallel to the directions indicated. The precision of the measurements is limited to about 0.05 by residual magnetic fields in the CRYOPAD.

Crystal	$hk.l$	Axis $\parallel z$	Axis $\parallel H$	Axis $\parallel E$	Incident polarization			Scattered polarization		
					$x$	$y$	$z$	$x$	$y$	$z$
I	$\bar{1}0.2$	01.0	00.1	00.1	0.00	0.00	0.88	0.83	0.06	0.08
		$0\bar{1}.0$	$00.\bar{1}$	$00.\bar{1}$	0.00	0.00	0.72	-0.69	0.06	-0.06
		$0\bar{1}.0$	00.1	$00.\bar{1}$	0.00	0.00	0.72	0.71	0.12	0.02
		$0\bar{1}.0$	00.1	00.1	0.00	0.00	0.72	-0.70	0.05	-0.05
		$0\bar{1}.0$	$00.\bar{1}$	00.1	0.00	0.00	0.72	0.70	0.16	0.05
II	$10.\bar{2}$	$0\bar{1}.0$	$00.\bar{1}$	$00.\bar{1}$	0.00	0.00	0.88	-0.87	0.03	0.02
		$0\bar{1}.0$	$00.\bar{1}$	$00.\bar{1}$	0.88	0.00	0.00	-0.10	0.00	0.86
		$0\bar{1}.0$	$00.\bar{1}$	$00.\bar{1}$	0.00	0.88	0.00	0.06	0.88	0.03
		$0\bar{1}.0$	$00.\bar{1}$	00.1	0.00	0.00	0.88	0.86	0.12	0.14
		$0\bar{1}.0$	$00.\bar{1}$	00.1	0.88	0.00	0.00	0.12	0.00	-0.85
		$0\bar{1}.0$	$00.\bar{1}$	00.1	0.00	0.88	0.00	0.00	0.88	-0.05
II	$\bar{1}0.2$	$0\bar{1}.0$	$00.\bar{1}$	00.1	0.00	0.00	0.88	0.87	0.03	0.08
		$0\bar{1}.0$	$00.\bar{1}$	00.1	0.88	0.00	0.00	0.10	0.06	-0.86
		$0\bar{1}.0$	$00.\bar{1}$	00.1	0.00	0.88	0.00	-0.09	0.88	0.02

Table 2 gives the components of scattered polarization measured for several different crystals, field directions and orientations. These results show that when the electric and magnetic fields were parallel to one another and to  $\pm c$ , the  $\bar{1}0.2$  reflection rotated polarization incident parallel to  $+z$  ( $[01.0]$ ) towards  $+x$  ( $\bar{1}0.2$ ). With  $[0\bar{1}.0]$  parallel to  $+z$  and parallel fields the rotation was towards  $-x$  ( $10.\bar{2}$ ). When the electric and magnetic fields were opposed the direction of rotation was reversed. It can be seen from the polarization given by equation (7) that when the sample was cooled in parallel fields the domain for which  $\gamma q_y$  is negative is stabilized. The nuclear structure factor for the  $\bar{1}0.2$  reflection is  $-2.51 \times 10^{-12} \text{ cm}$  and the factor  $\sin(2\pi \ell z) = -0.976$ . Using equation (1) this gives

$$\gamma = 0.976 \times 12M_{\text{Cr}}f_{\text{Cr}}(\kappa)/2.51$$

which is positive. For  $\{h0.l\}$  reflections measured with  $[01.0]$  parallel to  $z$ ,  $q_y$  has the opposite sign to  $h$  and so is positive for  $\bar{1}0.2$ . To make  $\gamma q_y$  negative  $M_{\text{Cr}}$  must be negative which implies that the moment on the Cr1 sites points along  $-c$ . The domain stabilized by parallel fields is therefore that in which the two moments in each double-octahedral complex point towards one another and towards the common triangle of  $\text{O}^{2-}$  ligands (figure 2).

## 6. The atomic origin of the ME effect

A phenomenological theory which describes the temperature dependence of the ME coefficients of antiferromagnets has been developed by Rado [13] for  $\text{Cr}_2\text{O}_3$ . The ME

tensor  $\alpha$  is defined by the relationship

$$B_i = \sum_{j=1}^{j=3} (\chi_{ij} H_j + \alpha_{ij} E_j)$$

where  $\chi_{ij}$  is the magnetic susceptibility. For Cr<sub>2</sub>O<sub>3</sub> which is uniaxial,  $\alpha$  has just two components  $\alpha_{\parallel}$  and  $\alpha_{\perp}$ , so

$$B_{\parallel} = \chi_{\parallel} H_{\parallel} + \alpha_{\parallel} E_{\parallel} \quad \text{and} \quad B_{\perp} = \chi_{\perp} H_{\perp} + \alpha_{\perp} E_{\perp}.$$

Rado introduces a fictitious magnetic field  $\mathbf{h}$  such that the magnetization produced by  $\mathbf{h}$  is identical to that produced by the electric field. This definition leads to

$$\alpha_{\parallel} = 4\pi M_{\parallel} / E_{\parallel} = 4\pi \chi_{\parallel} h_{\parallel} / E_{\parallel}.$$

He conjectures that  $h_{\parallel}$  has the form

$$h_{\parallel} = a_{\parallel} E_{\parallel} \langle S_z \rangle_{av}$$

and hence that

$$\alpha_{\parallel} = 4\pi a_{\parallel} \chi_{\parallel} \langle S_z \rangle_{av}$$

where  $a_{\parallel}$  is a temperature-independent constant of the material. There are analogous expressions for the perpendicular components. In this phenomenological theory the magnetoelectric coefficients are proportional to the magnetic susceptibility and to the sublattice magnetization and so go to zero at the Néel temperature, as observed. In addition, when the magnetic moment is parallel to  $z$ , the parallel component  $\alpha_{zz} = \alpha_{\parallel}$  should tend to zero with the susceptibility  $\chi_{\parallel}$  as  $T \Rightarrow 0$ . In general this theory reproduces the different temperature dependencies of  $\alpha_{\parallel}$  and  $\alpha_{\perp}$  quite well, although in Cr<sub>2</sub>O<sub>3</sub>  $\alpha_{\parallel}$  drops to zero at around 100 K and has a finite value at low temperatures [3], so it is not universally applicable.

There have been three basically different atomic mechanisms proposed for ME effects. Rado [13] suggests that the atomic origin of  $\mathbf{h}$  is an extra term in the spin Hamiltonian with the form  $\pm g \mu_B a S_z^2 E$  where  $g$ ,  $\mu_B$  and  $S_z$  denote, respectively, the spectroscopic splitting factor, the Bohr magneton and the operator giving the  $z$ -component of the spin. In this single-ion theory the ME effect arises from the fourth-order electric field dependence of the spin-orbit splitting of the atomic levels. In the two-ion theory [14] the parallel ME effect is linked to the magnetic susceptibility through the field dependence of the isotropic exchange interaction. In the third mechanism, which is thought to be of prime importance in rare-earth antiferromagnets, the ME effect arises as a result of the direct effect on the atomic magnetic moments of an electric field dependence of the spectroscopic splitting tensor  $\mathbf{g}$  [15, 16].

## 7. The mechanism for magnetic annealing

The process by which the simultaneous application of a magnetic and an electric field during the cooling of a sample through the Néel temperature favours the nucleation of a single 180° domain should be understandable in terms of the processes which have been invoked to account for the ME effect. In the present case in which the electric and magnetic fields  $E_z$  and  $H_z$  are parallel to the [00.1] direction in Cr<sub>2</sub>O<sub>3</sub> it is assumed that the first-order effect of the applied electric field will be to shift the Cr<sup>3+</sup> cation with respect to its anion ligands a small distance along the  $c$ -axis in the direction of the field. The spin Hamiltonian for the paramagnetic phase in the absence of an electric field has the form

$$H_z S_x \mu_B g_{\parallel} + 2D(S_z^2 - \frac{1}{3}S(S+1))$$



in which  $g_{\parallel} = \lambda/\Delta$  where  $\lambda$  is the spin-orbit coupling coefficient and  $\Delta$  the cubic crystal-field splitting energy;  $D$  gives the magnitude of the quadrupole term in the splitting of the ground-state multiplet. The spin Hamiltonian given above is modified by applying an electric field and can then be written as

$$H_z S_x \mu_B \left( g_{\parallel} \pm \frac{\partial g_{\parallel}}{\partial z} \frac{\partial z}{\partial E_z} E \right) + 2 \left( D \pm \frac{\partial D}{\partial z} \frac{\partial z}{\partial E} E \right) \left( S_z^2 - \frac{1}{3} S(S+1) \right)$$

where the plus signs correspond to one set of  $\text{Cr}^{3+}$  sites, say A, and the minus signs to the set of centrosymmetrically related sites B. For  $\text{Cr}^{3+}$ ,  $S = \frac{3}{2}$  and the energy levels of the ground-state quadruplet become

$$\begin{array}{ll} \frac{3}{2} H \mu_B (g_{\parallel} \pm \delta g_{\parallel}) + (D \pm \delta D) & \frac{1}{2} H \mu_B (g_{\parallel} \pm \delta g_{\parallel}) - (D \pm \delta D) \\ -\frac{1}{2} H \mu_B (g_{\parallel} \pm \delta g_{\parallel}) - (D \pm \delta D) & -\frac{3}{2} H \mu_B (g_{\parallel} \pm \delta g_{\parallel}) + (D \pm \delta D) \end{array}$$

where

$$\delta g_{\parallel} = \frac{\partial g_{\parallel}}{\partial z} \frac{\partial z}{\partial E_z} E \quad \text{and} \quad \delta D = \frac{\partial D}{\partial z} \frac{\partial z}{\partial E} E.$$

The presence of simultaneous electric and magnetic fields will unbalance the populations of these different spin states at the A and B sites in the paramagnetic phase, favouring configurations in which more spins are parallel to  $\mathbf{H}$  at the A sites. Note however that in the paramagnetic state the imbalance is entirely due to the term in  $\delta g$ . As the phase transition progresses the combined effect of the fields is to reduce the energy of an antiferromagnetically ordered nucleus of  $2N$  cations with  $S_z = \frac{3}{2}$  at the A sites and  $S_z = -\frac{3}{2}$  at the B sites, below that for the reverse configuration, by  $3NH \delta g_{\parallel} E$ . Formation of a single domain therefore becomes probable if  $H \delta g_{\parallel} E \approx kT_N$ . In order to determine which is the A and which is the B site it is necessary to look more closely at the mechanisms proposed in the previous section.

The effect of the odd components of the crystal field on the wave-functions of magnetic ions have been shown by [17] to add terms of the form  $\langle g | V_{cr}^u | u \rangle \langle u | V_{cr}^u | g' \rangle / \Delta$  to terms such as  $\langle g | V_{cr}^s | g' \rangle$ . Here  $|u\rangle$  and  $|g\rangle$  are odd and even basis functions and  $V_{cr}^u$  and  $V_{cr}^s$  the odd and even parts of the crystal electric field respectively. An external applied electric field will increase the magnitude of these extra terms at one site and decrease them at the centrosymmetrically related one. The way in which both  $\mathbf{g}$  and the spin-orbit splitting depend on the electric field through the perturbation of the ground-state splitting parameters by these electric-field-dependent terms has been investigated [15, 18]. However, fitting a purely electrostatic model of the crystal field to the spectroscopic data leads to unrealistic values of the adjustable parameters of the model. A molecular orbital model in which covalent effects are taken into account explicitly can remove some of these difficulties [18]. The ground-state splitting parameters  $\Delta$  and  $D$  for  $\text{Cr}^{3+}$  in ruby have been calculated using a semi-empirical LCAO method [19]. The calculation was carried out for the equilibrium configuration of the  $\text{CrO}_6$  complex and for configurations which might result from application of an axial electric field—in which the  $\text{Cr}^{3+}$  ions were shifted along the [00.1] direction first towards (+ shift) and then away from (− shift) their large close triangle of oxygen neighbours. The effect of a positive shift was to decrease  $\Delta$  and increase  $-D$ , but with the proportional change in  $D$  nearly ten times greater than that in  $\Delta$ . Similar but opposite changes were found for a negative shift. The  $\mathbf{g}$  tensor for  $\text{Cr}^{3+}$  ions is given in terms of the ground-state splitting parameters as

$$g_{\parallel} = 2 - 8\lambda/(\Delta + \epsilon) \quad \text{and} \quad g_{\perp} = 2 - 8\lambda/(\Delta - \epsilon) \quad (8)$$

where  $\lambda$  is the spin-orbit parameter and  $\epsilon = \Delta^2 D / 8\lambda^2$  [20]. The effect of an electric field applied parallel to [00.1] is to shift the  $\text{Cr}^{3+}$  ions along the  $c$ -axis relative to their coordinating oxygen neighbours. The  $\text{Cr}^{3+}$  ion whose  $z$ -coordinate is 0.3476 (Cr1) moves towards the triangle formed by its three closest neighbours whereas the shift of that with  $z = 0.6524$  (Cr2) takes it further from its equivalent triangle. Using equation (8), the change in the effective spin of Cr1 due to the  $g$ -factor mechanism is

$$\frac{\partial g_{\parallel}}{\partial z} \mu_B S_z \approx \frac{8\lambda^2}{\Delta^2} \frac{\partial \Delta}{\partial z}$$

which has been shown to be negative [19]. From this it follows that  $\delta g_{\parallel}$  is negative at the Cr1 sites which should therefore be B sites (those with spins antiparallel to [00.1]) in the favoured domain. This is in fact the result that was obtained in the experiments.

## 8. Conclusion

It has been shown that the type of domain stabilized by cooling in parallel electric and magnetic fields is that in which the magnetic moments on the  $\text{Cr}^{3+}$  ions point towards the centre of the smaller triangle of ligand oxygens. The ME mechanism which is most effective in stabilizing a particular magnetic domain during the magnetic annealing process is probably the  $g$ -factor effect [15]. Both the spin-orbit effect [13] and the antisymmetric exchange coupling effect [14] give energy splittings proportional to the sublattice magnetizations, and these therefore tend to zero at the Néel point. The effect on the stability of the domains of cooling in a magnetic field only is not so easy to understand. It is probably associated with defects in the crystal leading to internal strains giving local piezoelectric effects. This would explain why the phenomena are crystal dependent, irreversible, and not completely reproducible.

The magnetoelectric coefficients predicted for the  $g$ -factor and spin-orbit mechanisms for the same domain are supposed to have opposite signs, and this has been invoked to account for the change in sign of  $\alpha_{\parallel}$  at around 100 K [16]. Our results probably imply that the domain stabilized by parallel electric and magnetic fields is that which gives a negative  $\alpha_{\parallel}$  in the high-temperature region.

## Acknowledgments

We would like to thank E Lelièvre-Berna and E Bourgeat-Lami for their help in setting up CRYOPAD II.

## References

- [1] Landau L D and Lifshitz E M 1960 *Electrodynamics of Continuous Media* (New York: Addison-Wesley) p 119
- [2] Dzyaloshinskii I E 1960 *Sov. Phys.-JETP* **10** 628
- [3] Astrov D N 1960 *Sov. Phys.-JETP* **13** 729
- [4] Folen V J, Rado G T and Stalder E W 1961 *Phys. Rev. Lett.* **6** 607
- [5] Lal H B, Srivastava R and Srivastava K G 1967 *Phys. Rev.* **154** 505
- [6] Martin T J and Anderson J C 1964 *Phys. Lett.* **11** 109
- [7] Rado G T and Folen V J 1961 *Phys. Rev. Lett.* **7** 310
- [8] Tasset F, Brown P J and Forsyth J B 1988 *J. Appl. Phys.* **63** 3606
- [9] Brockhouse B N 1953 *J. Chem. Phys.* **21** 961
- [10] Nathans R, Riste T, Shirane G and Shull C G 1958 *MIT Structure of Solids Group Technical Report No 4*

- [11] Blume M 1963 *Phys. Rev.* **130** 1670
- [12] Brown P J, Forsyth J B and Tasset F 1993 *Proc. R. Soc. A* **442** 147
- [13] Rado G T 1961 *Phys. Rev. Lett.* **6** 609
- [14] Date M, Kanamori J and Tachiki M 1961 *J. Phys. Soc. Japan* **16** 2589
- [15] Alexander S and Shtrikman S 1966 *Solid State Commun.* **4** 115
- [16] Rado G T 1969 *Phys. Rev. Lett.* **23** 644
- [17] Artman J O and Murphy J C 1962 *Bull. Am. Phys. Soc.* **7** 196
- [18] Royce E B and Bloembergen N 1963 *Phys. Rev.* **131** 1912
- [19] Lohr L L and Lipscomb W N 1963 *J. Chem. Phys.* **38** 1607
- [20] Abragam A and Bleaney B 1970 *Electron Paramagnetic Resonance of Transition Metal Ions* (Oxford: Oxford University Press) p 431